Published in final edited form as:
Indian J Biochem Biophys. 2013 October ; 50(5): 411–418.

Analysis of osmotic stress-induced Ca^{2+} spark termination in mammalian skeletal muscle

Christopher Ferrante[1], **Henrietta Szappanos**[1], **László Csernoch**[2], and **Noah Weisleder**[3,*]

[1]Department of Physiology and Biophysics, Robert Wood Johnson Medical School, 675 Hoes Lane Piscataway, NJ 08854, USA

[2]Department of Physiology, Medical and Health Science Center, University of Debrecen, Nagyerdei krt. 98, Debrecen, Hungary

[3]Department of Physiology and Cell Biology, Davis Heart and Lung Research Institute, The Ohio State University Wexner Medical Center, 473 W 12th Ave, Columbus, OH 43210, USA

Abstract

Ca^{2+} sparks represent synchronous opening of the ryanodine receptor (RyR) Ca^{2+} release channels located at the sarcoplasmic reticulum (SR) membrane. Whereas a quantal nature of Ca^{2+} sparks has been defined in cardiac muscle, the regulation of Ca^{2+} sparks in skeletal muscle has not been well studied. Osmotic-stress applied to an intact skeletal muscle fiber can produce brief Ca^{2+} sparks and prolonged Ca^{2+} burst events. Here, we show that termination of Ca^{2+} bursts occurs in a step wise and quantal manner. Ca^{2+} burst events display kinetic features that are consistent with the involvement of both stochastic attrition and coordinated closure of RyR channels in the termination of SR Ca^{2+} release. Elemental unitary transition steps could be defined with a mean $\Delta F/F_0$ of ~0.28, corresponding to the gating of 1–2 RyR channels. Moreover, the amplitude of the elemental transition steps declines at the later stage of the burst event. In tandem Ca^{2+} burst events where two Ca^{2+} bursts occur at the same position within a fiber in rapid succession, the trailing event is consistently of lower amplitude than the initial event. These two complementary results suggest that SR Ca^{2+} release may be associated with local depletion of SR Ca^{2+} stores in mammalian skeletal muscle.

Keywords

calcium; Ca^{2+}; sparks; calcium induced calcium release; sarcoplasmic reticulum; skeletal muscle; termination

Introduction

The calcium ion (Ca^{2+}) acts as a vital second messenger in many cell types influencing myriad cellular processes, including contraction of muscle fibers. Release of sequestered Ca^{2+} from the sarcoplasmic reticulum (SR) through ryanodine receptor (RyR) channels constitutes the major signal driving excitation-contraction (E-C) coupling in muscle cells. In

*Author correspondence to: Tel: +0 1 (614) 292-5321, Fax: +0 1 (614) 247-7799, noah.weisleder@osumc.edu.

skeletal, cardiac and smooth muscle the elemental components of SR Ca^{2+} release are discrete, localized units known as Ca^{2+} sparks[1–5]. These Ca^{2+} release events originate from highly structured paracrystalline arrays of RyR channels in the SR[6–8].

While spontaneous Ca^{2+} sparks ensure rhythmic contractile activity of the cardiac muscle, in skeletal muscle, SR Ca^{2+} release must be tightly repressed during the resting state, capable of rapid activation upon arrival of action potential stimulation and promptly terminate to end contraction. Initial studies detecting Ca^{2+} sparks in skeletal muscle have been performed with amphibian muscle[2]. Ca^{2+} sparks are also detected in embryonic mammalian skeletal muscle[9], where they are attributed to the presence of the type 3 RyR (RyR3), the dominant RyR isoform at this stage of development[10,11]. While rare observations of Ca^{2+} sparks have been made in resting intact mammalian fibers[9,11], until recently biophysical studies of Ca^{2+} sparks in mammalian skeletal muscle were generally performed with fibers where the sarcolemma is disrupted through various physical or chemical skinning methods[12–14].

Our laboratory has determined that stress generated by membrane deformation induces a fluttered SR Ca^{2+} release response that is confined to the periphery of the intact mammalian muscle fibers[15–17]. These events originate from RyR1 using pharmacological inhibition and experiments in knockout mouse models for RyR3. These events are also dependent on activation of the Type 1 inositol (1,4,5)-trisphosphate receptor for activation of this response[18]. In addition to the short Ca^{2+} release events that resemble Ca^{2+} sparks observed in cardiac and permeabilized skeletal muscles, a distinct population of prolonged Ca^{2+} burst events is generated in intact skeletal muscle fibers following osmotic shock.

The slow, asynchronous termination of Ca^{2+} bursts provide a unique case to investigate the coordination of RyR closure and the mechanisms that influence SR Ca^{2+} release termination. Through kinetic analysis of these Ca^{2+} burst events, we now present evidence to support a quantal nature of SR Ca^{2+} release termination in intact mammalian skeletal muscle. As quantal SR Ca^{2+} release has been observed in cardiomyocytes[19], characterization of the elemental units of SR Ca^{2+} release in both skeletal and cardiac muscles should provide insight into the regulatory processes of Ca^{2+} signaling in muscle and cardiovascular physiology.

Methods

Induction of Ca^{2+} sparks and Ca^{2+} bursts

Ca^{2+} sparks were induced using previously established techniques[20]. Male C57Bl6/J mice, aged 8–12 weeks, were maintained under conditions in agreement with local regulation with regulated light cycles and standard rodent diet. Mice were sacrificed by cervical dislocation and flexor digitorum brevis (FDB) muscles were surgically removed in an isotonic balanced salt solution (Tyrode) consisting of the following 140 mM NaCl, 5 mM KCl, 2.5 mM $CaCl_2$, 2 mM $MgCl_2$, 10 mM HEPES (pH 7.2), with a measured osmolarity of 290 mOsm. Muscles were digested in the same solution supplemented with 2 mg/ml type I collagenase (Sigma C-0130, St. Louis, MO) for 55 min at 37°C.

Following collagenase treatment, FDB muscles were washed twice by immersion in Tyrode buffer and then gently dissociated by several passages through a series of pipettes with decreasing diameter. Fibers were plated on ΔTC3 glass-bottomed dishes (Bioptechs, Butler, PA) in Tyrode and immediately loaded with 10 μM Fluo-4-AM Ca^{2+} indicator (Molecular Probes, Eugene, OR) for 60 min at room temperature. Excess Fluo-4-AM was removed by washing four-times by replacing half the volume of the dish with fresh Tyrode. All muscle fibers used in analysis were confirmed to have intact sarcolemmal membranes and regular striation patterns by phase-contrast microscopy and were used within 6 h after Fluo-4 loading. Selected fibers were perfused with Tyrode buffer from a fast flow perfusion system until measurements began. Cell swelling was induced by perfusion with a hypotonic solution containing 50 mM NaCl, 5 mM KCl, 2.5 mM $CaCl_2$, 2 mM $MgCl_2$, 10 mM HEPES (pH 7.2), with a measured osmolarity of 170 mOsm. After 60–180 s exposure to hypotonic solution, cells were perfused with isotonic Tyrode to allow a return to normal cell volume. Measurements of Fluo-4 fluorescence on a 512 × 512 pixel panel were performed on a Radiance-2100 confocal microscope (BioRad, Hercules, CA) with an argon laser (488 nm) and a 40×, 1.3NA oil immersion objective (Nikon, Melville, NY). Line-scan images were acquired at a sampling rate of 2 ms per line and serial X-Y images of muscle fibers were acquired at 3.08 s per frame. Data analysis was performed using IDL software with custom routines[16,17].

Kinetic analysis of the termination of Ca^{2+} sparks and Ca^{2+} bursts

Because of the heterogeneity of Ca^{2+} spark responses that followed an osmotic shock in intact muscle fibers, traditional methods of Ca^{2+} spark image analysis were modified to accommodate the kinetic analysis of the Ca^{2+} spark and Ca^{2+} burst populations. Three major modalities of analysis were employed in this study.

First, a semi-automatic user-directed imaging program was used to identify localized Ca^{2+} release events in line-scan measurements. Due to the semi-automatic nature of the analysis event frequencies were not determined. To define a Ca^{2+} burst event, Ca^{2+} transients with durations longer than 400 ms that were spatially confined to 5 μm width and a peak amplitude value of at least 0.5 $\Delta F/F_0$ were considered. These criteria essentially distinguish Ca^{2+} bursts from the ember events found in previous studies with permeabilized mammalian muscle[12–14]. Second, whenever possible, exponential functions were used to derive the time constant for termination of Ca^{2+} spark events that exhibit apparent monophasic decay. This analysis was mainly used to compare the kinetics of brief Ca^{2+} sparks and prolonged Ca^{2+} bursts. Third, for events with stepwise transitions amplitude histograms were used to resolve the distinct transition steps within a Ca^{2+} burst event. For this analysis, the mean $\Delta F/F_0$ for each point (2 ms) of an event was calculated and imported into Origin software (OriginLab) for graphic analysis. Raw $\Delta F/F_0$ values were smoothed by Fast Fourier-Transformation using a value of 20 points as a smoothing criterion. All smoothed $\Delta F/F_0$ values from the Ca^{2+} burst peak to the return to baseline were ordered into 0.025 bins and the resulting histogram was fit with the sum of multiple Gaussian functions:

$$f(x)=\sum_{i=0}^{N_{step}} A_i \bullet e^{\frac{-(x-x_i)^2}{\sigma_i^2}} \quad (1)$$

where A_i, x_i and σ_i are the magnitude, position and spread of the *i*th Gaussian. From this analysis, the number of steps within a discrete Ca^{2+} release event (N_{step}) and the magnitude of the unitary transition step (UTS = $x_{i+1} - x_i$) can be derived. Events were considered not to display stepwise closure when distinct peaks, periodic no-zero and zero values were not found in the histograms. This analysis was expanded to tandem Ca^{2+} burst events that occurred in rapid succession at the same position, where fitting with Gaussian distributions allowed the comparison of changes in N_{step} and UTS between the initial and trailing events.

Results

Ca^{2+} sparks and Ca^{2+} bursts in intact mammalian skeletal muscle fibers

While Ca^{2+} sparks are rarely observed in intact mammalian skeletal muscle fibers, such events can be induced in normal quiescent fibers by stress generated by varying the osmolarity of the extracellular solution[16]. These SR Ca^{2+} release events were generally localized to the periphery of the muscle fiber (Fig. 1a).

Three populations of Ca^{2+} release events were observed in this response. The first group includes short duration Ca^{2+} sparks that displayed rapid initiation and rapid termination of Ca^{2+} release with a mean $\tau = 62.8 \pm 9.0$ ms. The second group showed rapid initiation and termination kinetics very similar to those seen in the first group, but the duration of Ca^{2+} release was much greater ($\tau = 429 \pm 10.0$ ms) (Fig. 1b). In addition to the above groups, a distinct population of events displayed prolonged Ca^{2+} transients that showed similar activation kinetics, but terminated in a stepwise fashion, rather than terminating rapidly. Some Ca^{2+} sparks and Ca^{2+} bursts could originate from the same location (Fig. 1), suggesting that the differential kinetics of these two populations reflected either varying gating of SR Ca^{2+} release channels or alteration of SR Ca^{2+} uptake and intracellular Ca^{2+} buffering capacity within the muscle fiber.

The width of Ca^{2+} bursts remained spatially restricted during prolonged Ca^{2+} release. In addition, the time constant of decay in Ca^{2+} bursts could be as rapid as in Ca^{2+} sparks (Fig. 1c and d), suggesting that prolonged Ca^{2+} bursts did not result from alterations in intracellular Ca^{2+} buffering or Ca^{2+} clearance machinery, rather they reflected a different gating property of RyR-mediated SR Ca^{2+} release.

Quantal nature for termination of Ca^{2+} bursts in skeletal muscle

While some Ca^{2+} bursts displayed rapid termination kinetics, the majority of Ca^{2+} bursts terminated in an apparent stepwise fashion (Fig. 1d, **right panel**). Individual Ca^{2+} burst events were thus analyzed to determine if discrete steps could be resolved during the termination of Ca^{2+} release (Fig. 1d **and** 2a). Histograms of hundreds of amplitude data points were generated for multiple individual Ca^{2+} burst events were fitted with Gaussian functions allowing the program to determine the position (x_i) and width (σ_i) of each peak

(Eqn. 1). Clearly, distinct transition steps could be resolved within the majority (~60%) of Ca^{2+} burst events, as shown in Fig. 2b.

Analysis of the distances between neighboring peaks ($x_{i+1} - x_i$) allowed the resolution of the unitary transition steps (UTS) for the event. Furthermore, both UTS and σ_i were found to be close to independent of i, indicating that indeed elementary steps of channel closure were resolved. However, two deviations from this equally spaced pattern of x_i were found. First, UTS seemed to be slightly larger at greater *i*. This finding will be examined in more detail later. Second, in a subset of Ca^{2+} burst events, large UTS were observed that sometimes coincided with an increased σ_i, suggesting a contribution from adjacent transitions. Careful examination of these large UTS revealed that they were multiples of other UTS determined from the same histogram, indicating a co-operative gating behavior of RyR Ca^{2+} release channels. In these events, N_{step} was calculated with the notion that in Eqn. 1 A_i could be zero for a certain *i*.

Since the UTS amplitude did vary with the number of transitions, an average unitary transition step was obtained by dividing the peak $\Delta F/F_0$ of the event with N_{step} for each individual burst. Plotting the frequency of average UTS values in the data set revealed an approximate Gaussian distribution with a mean value of $\Delta F/F_0 = 0.283 \pm 0.004$ (Fig. 2c). Additional analysis revealed that the occurrence for the N_{step} values for individual events followed a Poisson distribution, as would be expected considering a stochastic nature of RyR opening (Fig. 2d). The close match of our data with the predicted Poisson distribution helps to validate our selection criteria and analysis as unbiased.

If a continuous supply of Ca^{2+} was maintained during the course of Ca^{2+} bursts, one expected a linear relationship between UTS amplitude at corresponding N_{step} values. It is well-known that local SR Ca^{2+} concentration plays an important role in maintaining Ca^{2+} release, as previous studies have hypothesized[21–23] or directly shown that local Ca^{2+} depletion influences SR Ca^{2+} release during Ca^{2+} sparks in cardiomyocytes[24] and permeabilized amphibian skeletal muscle fibers[25]. Since this local depletion of SR Ca^{2+} stores has not been previously observed in intact mammalian skeletal muscle, we examined if the local SR Ca^{2+} load modulated the activation or termination of Ca^{2+} release from the SR during extended Ca^{2+} bursts[26,27]. By plotting all UTS values with the corresponding N_{step} value for multiple events, we found that UTS did not vary in a linear fashion with N_{step} (Fig. 2e). A linear relationship would be expected since Ca^{2+} bursts having a constant plateau, indicating that equilibrium was reached. In this case, deviation from a linear relationship could only result from reducing the current through individual RyR channels and forcing the curve downwards. Our observation of a significant upward deflection indicated that the amplitude of UTS during initial closing steps (higher N_{step}) was elevated above the expected values based on the UTS amplitude of the later closing steps. This non-linear relationship suggested that the amplitude of the each UTS decreased during the prolonged closing phase of a Ca^{2+} burst.

Multiple processes contribute to termination of Ca^{2+} bursts

The stepwise closing phase of Ca^{2+} bursts also displayed increases in Ca^{2+} that likely result from reopening of RyR channels that had closed or the initial opening of additional RyR

channels (Fig. 3a). Both opening and closing events during the decay phase could pass through multiple step levels (as mentioned earlier and see also Fig. 3a), suggesting that coupled gating of RyR channels could occur during the decay phase.

In addition to SR Ca^{2+} load, two other factors are thought to contribute to the rapid termination of Ca^{2+} sparks in muscle cells[21]; stochastic attrition and Ca^{2+}-dependent inactivation of RyR channel release. The distribution of the dwell time of first opening (τ_0) for each N_{step} is expected to follow a logarithmic decay curve

$$\tau_0 = \tau \bullet \ln\left(\frac{N}{N-1}\right) \quad (2)$$

where τ is the time constant of overall decay (1.28 ± 0.27 s), if only stochastic attrition controls the transition from the first to second level of Ca^{2+} release during a Ca^{2+} burst. In events with fewer steps (lower N_{step} values), measured τ_0 values closely matched values predicted to reflect stochastic RyR closing (Fig. 3b) in the data set that represented a variety of different τ_0 values (Fig. 3c). Interestingly, the only events that varied significantly from predicted stochastic values involved those with intermediate N_{step}. This could result from simultaneous RyR channel closings, either as a result of direct coupling of RyR closing, or by inactivation of adjacent RyR by local Ca^{2+} concentrations.

Local depletion of SR Ca^{2+} stores during prolonged Ca^{2+} release

Additional insight into the role of local SR Ca^{2+} store depletion came from analysis of Ca^{2+} burst events that originated from the same location in rapid succession. In such tandem events, the trailing burst was consistently reduced in amplitude compared to the initial burst (Fig. 4a). Resolution of individual steps within the decay phase of tandem events revealed that even at the same N_{step} values, the trailing burst displayed reduced step amplitude compared to the initiating burst (Fig. 4b). Examination of multiple tandem events established that the mean UTS in trailing bursts was significantly diminished when compared to initiating bursts (Fig. 4c), while the mean number of steps remained essentially the same (Fig. 4d). The maintenance of the number of discrete steps coupled with diminished amplitude of these steps suggested a reduction in the quantity of Ca^{2+} released by the same number of RyR channels. In this case, a local reduction of SR Ca^{2+} store would occur during the initial burst, resulting in less Ca^{2+} available for release during the trailing burst until the local Ca^{2+} store could be replenished.

Discussion

Since Ca^{2+} sparks and bursts constitute the elemental units of SR Ca^{2+} release in skeletal muscle cells, a precise understanding of the nature of these individual Ca^{2+} release events will greatly contribute to determining fundamental mechanisms that maintain Ca^{2+} homeostasis in skeletal muscle health and disease. This study establishes that the prolonged termination phase of Ca^{2+} bursts display a quantal nature. Characterization of these transition steps suggests that mostly stochastic attrition as well as coordinated gating underlie the closing of RyR channels. The rapid decline observed in Ca^{2+} sparks and some Ca^{2+} bursts likely results from Ca^{2+}-dependent inactivation of RyR channels and is thus

distinct from the prolonged, step-wise decline present in other Ca^{2+} bursts. Our findings suggest that local depletion of the Ca^{2+} store during prolonged Ca^{2+} bursts results in decreased amplitude, particularly during tandem Ca^{2+} bursts that originate from the same spatial position.

During the decay of Ca^{2+} bursts, the amplitude occasionally returns to a higher step (Fig. 3a), which likely results either from re-opening of RyR channels previously closed or the opening of additional RyR channels. The opening of additional RyR channels would likely result from propagating Ca^{2+}-induced Ca^{2+} release (CICR) within a cluster, however, stochastic or coordinated channel openings could also contribute. If CICR propagation contributes to RyR re-opening, this would suggest that RyR inactivation due to local elevated cytosolic Ca^{2+} levels could be overcome, perhaps by a combination of diminished SR Ca^{2+} release and clearance of Ca^{2+} from the cytosol. Furthermore, if this is the case, one would expect to see a prolonged restoration of Ca^{2+} release. As the duration of additional Ca^{2+} release tends to be brief, this suggests that both direct coupling and CICR are at work in skeletal muscle RyR arrays. It is possible that they are complementary in amplification of Ca^{2+} release in mammalian skeletal muscle.

A role for direct coupling of RyR channels within SR RyR arrays during termination of Ca^{2+} release is also supported by the finding that the τ_o value for events with an intermediate N_{step} is elevated above values projected for simple stochastic decay of RyR opening (Fig. 3b). It is interesting that it is the intermediate N_{step} events that do not meet this stochastic prediction. If it were short events with presumably less Ca^{2+} released that did not meet the stochastic prediction, then one might expect that the differences seen between a stochastic response and the observed values were due to insufficient Ca^{2+} present to produce Ca^{2+} inactivation. Or, if the events with high N_{step} resulted in non-stochastic closing one would assume that this was the result of spatial effects, where some RyR channels are exposed to higher levels of Ca^{2+} than other channels due to the large quantity of Ca^{2+} released. However, since it is the intermediate values that display non-stochastic closing, this suggests that other factors such as direct coupling or inherent differential gating properties of RyR channels must contribute to their closing in Ca^{2+} bursts.

The appearance of Ca^{2+} blinks or skraps, nanoscale depletions of the SR Ca^{2+} store associated with Ca^{2+} sparks, have been observed in mammalian cardiomyocytes[24] and permeabilized amphibian skeletal muscle fibers[25]. Our study presents two findings that suggest this is also the case in mammalian skeletal muscle. First, our observation of decreased amplitude in late stage UTS of prolonged Ca^{2+} burst argues that local depletion of the SR Ca^{2+} store can occur in skeletal muscle fibers. As the prolonged Ca^{2+} burst continues, Ca^{2+} release continues to terminate in a step wise pattern, however, the UTS amplitude appears to decrease slightly during the later steps (Fig. 2e). This slight decrease in UTS is unlikely to result from the closure of RyR channels, since closure of RyR would probably result in a much larger drop than the observed change in subsequent UTS. With the number of active RyR channels remaining the same, this decrease would depend on a diminished supply of Ca^{2+} to be released, as one would expect to see as a result of a locally diminished SR Ca^{2+} store. While our analysis cannot precisely establish the number of RyR channels that contribute to Ca^{2+} bursts, certain predictions can be made. Previous studies

from other laboratories allow us to establish that the mean UTS value obtained here, $\Delta F/F_0$ ~0.28, likely results from the opening of 1–2 RyR channels[13,19,28].

Second, we find that in Ca^{2+} busts that occur in tandem the trailing events are generally of lower peak amplitude than the initial burst, suggesting that during Ca^{2+} bursts the quantity of Ca^{2+} released not only decreases in quantal units, but also that a supplemental decay mechanism contributes. In this situation, the most likely mechanism at work is local decreases in the Ca^{2+} store available for release from SR. It is important to note, however, that additional factors such as altered sarcolemmal Ca^{2+} uptake or changes in intracellular Ca^{2+} buffering capacity could also contribute to the observations in this study. Further experimentation may reveal that this depletion could be linked to the activation of store-operated Ca^{2+} entry to replenish the SR Ca^{2+} store. It is interesting to note that dystrophic muscle displays both accelerated store-operated Ca^{2+} entry[29–32] and elevated Ca^{2+} spark activity[16,33].

A matter of central importance in muscle physiology and E-C coupling research is the mechanism involved in activation and termination of RyR channels. By resolving the step wise closure of Ca^{2+} bursts into discrete units, we provide evidence that the quantal nature of Ca^{2+} bursts is similar to that seen in Ca^{2+} sparks from cardiomyocytes[19]. Variation in the amplitude of UTS, and decreased UTS values in trailing tandem Ca^{2+} bursts suggest that local SR Ca^{2+} depletion occurs during the termination of these prolonged Ca^{2+} release events. Furthermore, we find evidence that direct coupling between RyR channels may supplement CICR in regulation of Ca^{2+} release from paracrystalline arrays of RyR channels in skeletal muscle. Determining the extent that these two mechanisms contribute to regulation of internal Ca^{2+} homeostasis would provide valuable insight into E-C coupling and provide guidance for developing treatments to affect numerous disorders involving Ca^{2+} dysregulation.

Acknowledgments

Research reported in this publication was supported by the National Institute of Arthritis and Musculoskeletal and Skin Diseases, part of the National Institutes of Health, under Awards R00-AR054793 and R01-AR063084. The content is solely the responsibility of the authors and does not necessarily represent the official views of the National Institutes of Health.

Abbreviations

$\Delta F/F_0$	amplitude
CICR	calcium-induced calcium release
E-C	excitation-contraction
FDB	flexor digitorum brevis
N_{step}	number of steps
x_i	position
RyR	ryanodine receptor

RyR1	ryanodine receptor type 1 RyR
RyR3	ryanodine receptor type 3 RyR
SR	sarcoplasmic reticulum
UTS	unitary transition step
σ_i	width

References

1. Nelson MT, Cheng H, Rubart M, Santana LF, Bonev AD, Knot HJ, Lederer WJ. Science. 1995; 270:633–637. [PubMed: 7570021]
2. Klein MG, Cheng H, Santana LF, Jiang YH, Lederer WJ, Schneider MF. Nature. 1996; 379:455–458. [PubMed: 8559251]
3. Cheng H, Lederer WJ, Cannell MB. Science. 1993; 262:740–744. [PubMed: 8235594]
4. Wier WG, ter Keurs HE, Marban E, Gao WD, Balke CW. Circ Res. 1997; 81:462–469. [PubMed: 9314826]
5. Tsugorka A, Rios E, Blatter LA. Science. 1995; 269:1723–1726. [PubMed: 7569901]
6. Franzini-Armstrong C, Protasi F, Ramesh V. Biophys J. 1999; 77:1528–1539. [PubMed: 10465763]
7. Yin CC, Lai FA. Nat Cell Biol. 2000; 2:669–671. [PubMed: 10980710]
8. Takekura H, Franzini-Armstrong C. Biophys J. 2002; 83:2742–2753. [PubMed: 12414707]
9. Shirokova N, Garcia J, Rios E. J Physiol. 1998; 512(Pt 2):377–384. [PubMed: 9763628]
10. Ward CW, Schneider MF, Castillo D, Protasi F, Wang Y, Chen SR, Allen PD. J Physiol. 2000; 525(Pt 1):91–103. [PubMed: 10811728]
11. Conklin MW, Barone V, Sorrentino V, Coronado R. Biophys J. 1999; 77:1394–1403. [PubMed: 10465751]
12. Csernoch L, Zhou J, Stern MD, Brum G, Rios E. J Physiol. 2004; 557:43–58. [PubMed: 14990680]
13. Kirsch WG, Uttenweiler D, Fink RH. J Physiol. 2001; 537:379–389. [PubMed: 11731572]
14. Zhou J, Brum G, Gonzalez A, Launikonis BS, Stern MD, Rios E. J Gen Physiol. 2003; 122:95–114. [PubMed: 12835473]
15. Ward CW, Lederer WJ. Nat Cell Biol. 2005; 7:457–459. [PubMed: 15867931]
16. Wang X, Weisleder N, Collet C, Zhou J, Chu Y, Hirata Y, Zhao X, Pan Z, Brotto M, Cheng H, Ma J. Nat Cell Biol. 2005; 7:525–530. [PubMed: 15834406]
17. Weisleder N, Ferrante C, Hirata Y, Collet C, Chu Y, Cheng H, Takeshima H, Ma J. Cell Calcium. 2007; 42:548–555. [PubMed: 17412417]
18. Tjondrokoesoemo A, Li N, Lin PH, Pan Z, Ferrante CJ, Shirokova N, Brotto M, Weisleder N, Ma J. J Biol Chem. 2013; 288:2103–2109. [PubMed: 23223241]
19. Wang SQ, Stern MD, Rios E, Cheng H. Proc Natl Acad Sci USA. 2004; 101:3979–3984. [PubMed: 15004280]
20. Weisleder N, Zhou J, Ma J. Methods Mol Biol. 2012; 798:395–410. [PubMed: 22130850]
21. Stern MD, Cheng H. Cell Calcium. 2004; 35:591–601. [PubMed: 15110149]
22. Sobie EA, Dilly KW, dos Santos Cruz J, Lederer WJ, Jafri MS. Biophys J. 2002; 83:59–78. [PubMed: 12080100]
23. Gyorke I, Gyorke S. Biophys J. 1998; 75:2801–2810. [PubMed: 9826602]
24. Brochet DX, Yang D, Di Maio A, Lederer WJ, Franzini-Armstrong C, Cheng H. Proc Natl Acad Sci USA. 2005; 102:3099–3104. [PubMed: 15710901]
25. Launikonis BS, Zhou J, Royer L, Shannon TR, Brum G, Rios E. Proc Natl Acad Sci USA. 2006; 103:2982–2987. [PubMed: 16473932]
26. Gyorke S, Fill M. Science. 1993; 260:807–809. [PubMed: 8387229]

27. Meissner G. Annu Rev Physiol. 1994; 56:485–508. [PubMed: 7516645]
28. Uttenweiler D, Kirsch WG, Schulzke E, Both M, Fink RH. Eur Biophys J. 2002; 31:331–340. [PubMed: 12202909]
29. Vandebrouck A, Ducret T, Basset O, Sebille S, Raymond G, Ruegg U, Gailly P, Cognard C, Constantin B. Faseb J. 2006; 20:136–138. [PubMed: 16254044]
30. Cully TR, Edwards JN, Friedrich O, Stephenson DG, Murphy RM, Launikonis BS. Am J Physiol Cell Physiol. 2012; 303:C567–C576. [PubMed: 22785116]
31. Zhao X, Moloughney JG, Zhang S, Komazaki S, Weisleder N. PLoS One. 2012; 7:e49862. [PubMed: 23185465]
32. Edwards JN, Friedrich O, Cully TR, von Wegner F, Murphy RM, Launikonis BS. Am J Physiol Cell Physiol. 2010; 299:C42–C50. [PubMed: 20427714]
33. Teichmann MD, Wegner FV, Fink RH, Chamberlain JS, Launikonis BS, Martinac B, Friedrich O. PLoS One. 2008; 3:e3644. [PubMed: 18982068]

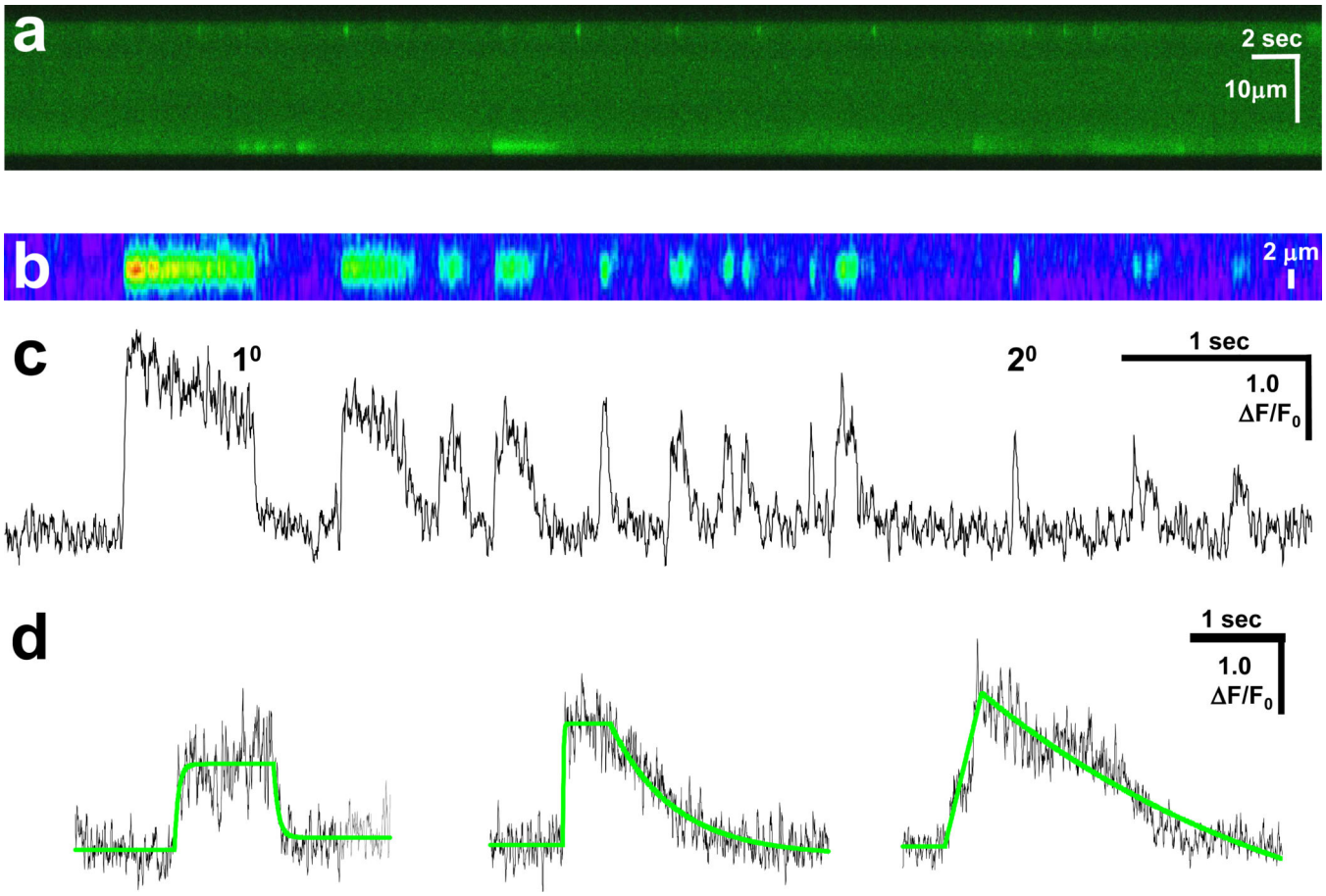

Fig 1. Osmotic shock induces Ca^{2+} sparks and Ca^{2+} bursts of varying duration

(**a**) Transverse line-scan of Fluo-4 loaded FDB fibers after osmotic shock revealed a robust response at the periphery of the fiber that included brief Ca^{2+} sparks and prolonged Ca^{2+} bursts; (**b**) Pseudo-colored magnified line-scan images from another fiber; (**c**) Unfiltered amplitude ($\Delta F/F_0$) trace of matching line-scan in panel **b**. Tracings reveal that the termination phase of Ca^{2+} bursts can occur in a rapid manner similar to Ca^{2+} sparks (**2^0**) and in a prolonged fashion (**1^0**). Both Ca^{2+} bursts and Ca^{2+} sparks can originate from the same location in a fiber; and (**d**) Representative unfiltered traces (**black**) of Ca^{2+} bursts displaying various termination kinetics. Single exponential curve fitting results are shown (**green line**).

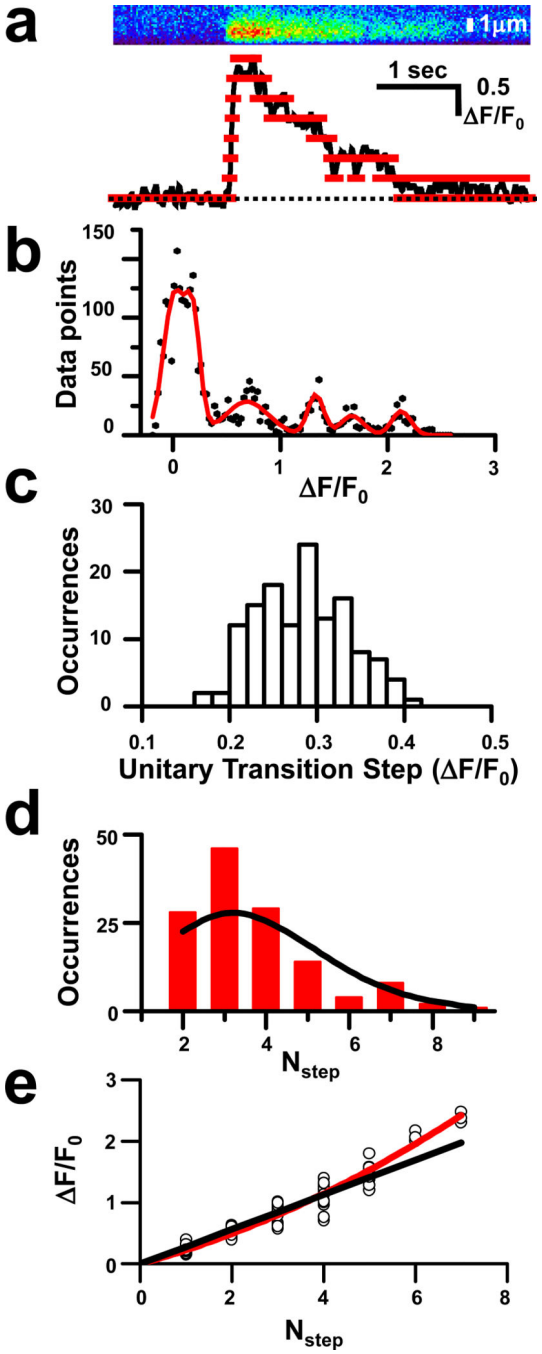

Fig 2. Decreased magnitude of quantal elements in termination of prolonged Ca^{2+} bursts

(**a**) Tracings (**bottom panel**) of smoothed data from line-scan data (**top panel**) reveal several steps (**red lines**); (**b**) Histogram of bin data for smoothed $\Delta F/F_0$ values fitted by multiple Gaussian functions (**red line**). Mean distance between the peaks determines the UTS amplitude. All peak distances in an event do not always match the standard UTS, as broader peaks likely contain contributions from adjacent transitions; (**c**) Distribution of the occurrence of given UTS values in the data set (n = 133), with a mean UTS of 0.283 ± 0.004 (mean ± SE). Such a range of UTS likely reflects slight deviation in data obtained from

confocal line scans, where the local plane of focus may slightly influence the signal recorded. The Gaussian distribution of this relationship suggests our data set is not biased towards events of high or low amplitude; (**d**) Distribution of the occurrence of events with a particular N_{step} value (**red bars**), with the predicted distribution indicated (**black line**). Predicted values are based on a Poisson distribution using the formula $P(n)=(\lambda^{n}*e^{-\lambda})/n!$, where λ is the mean value for the data set ($\lambda=3.67$); and (**e**) Plot of the amplitude ($\Delta F/F_0$) for each N_{step} value (**circle**) for multiple events (n=20) with a fit curve (**red line**) and line following the predicted value (**black line**) based on a regression line with a slope = 0.283 that passes through the origin.

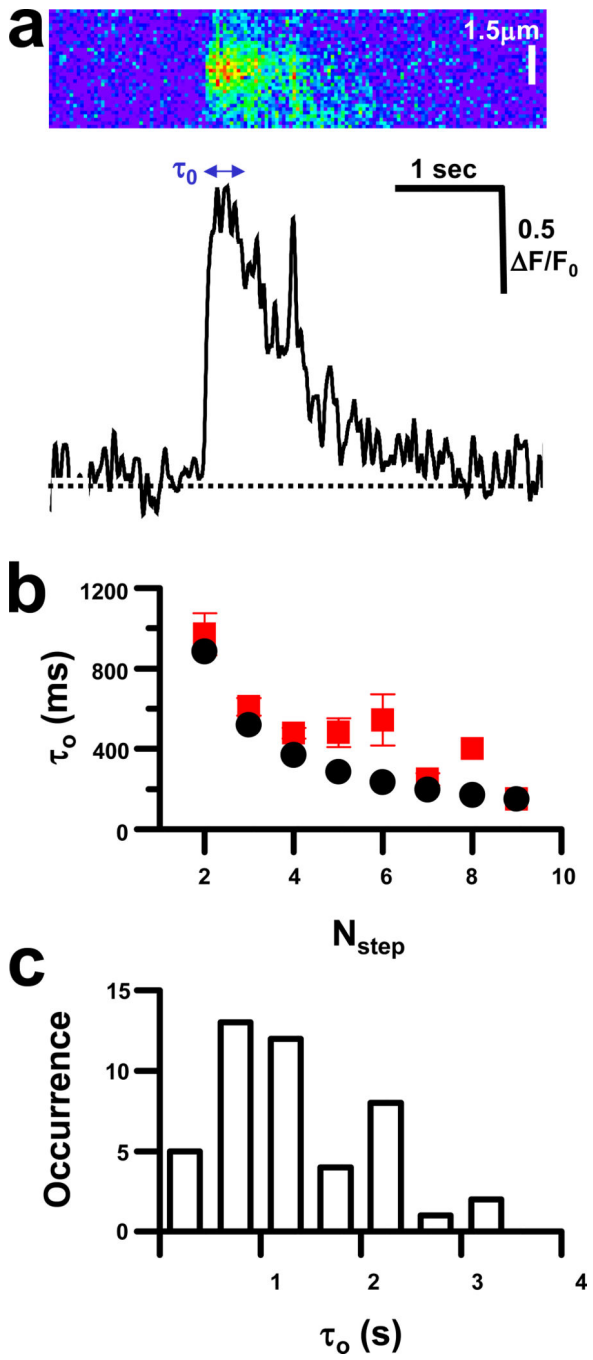

Fig 3. Coupling of RyR closure in Ca^{2+} burst termination

(**a**) Tracings (**bottom panel**) of line-scan images (**top panel**) reveal that Ca^{2+} release can briefly return to a previous step during the otherwise decreasing decay phase of Ca^{2+} bursts, sometimes returning to the same level as the initial opening; (**b**) Distribution of the mean duration of first opening (τ_0) for events with different number of steps (**red squares**). Stochastic closure of RyR channels would result in a decay curve displayed (Eqn. 2; **black circles**); and (**c**) Occurrence of different τ_0 in the complete data set.

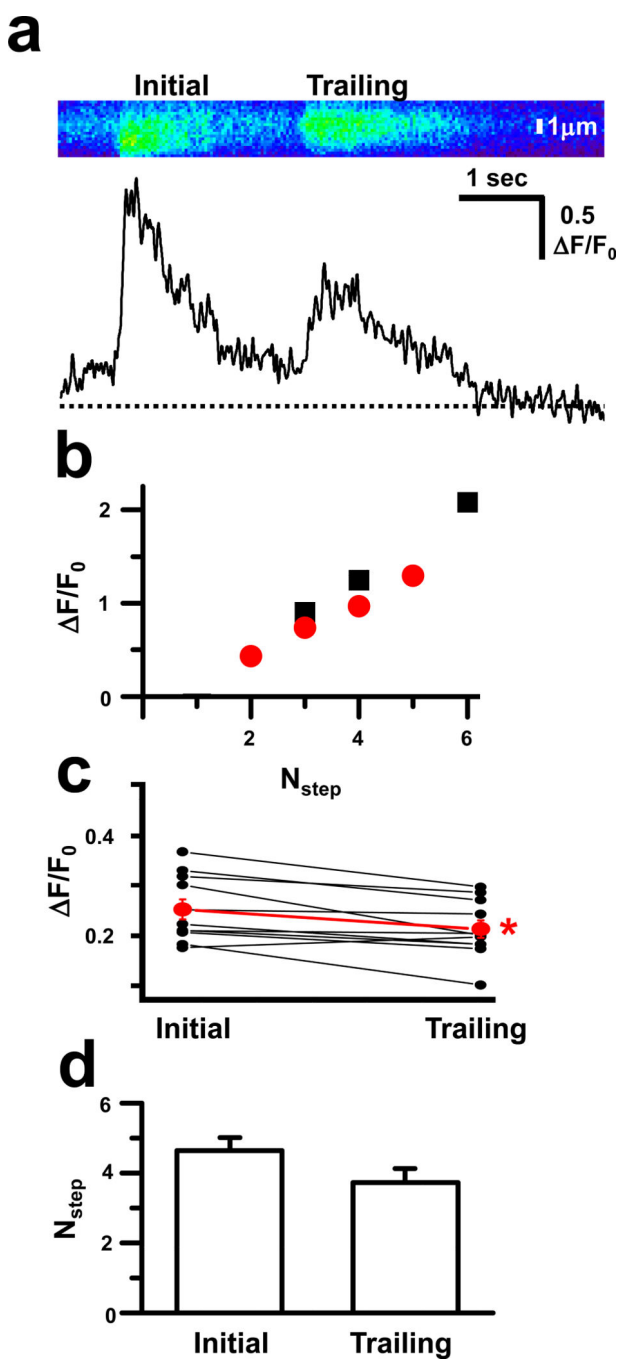

Fig 4. Tandem Ca^{2+} bursts reveal local depletion of SR Ca^{2+} stores

(**a**) Line-scan analysis (**top panel**) suggests that when Ca^{2+} bursts occur in rapid succession at the same location, the peak amplitude (**bottom panel**) is decreased in the trailing event; (**b**) Individual steps within the decay phase of a single tandem event with the amplitude for the initial (**black squares**) and trailing (**red circles**) bursts at matching N_{step} values; (**c**) Amplitude for initial step for both the initial and trailing Ca^{2+} bursts for several (n = 16) tandem events. Mean ± SE presented in **red**. * $p<0.05$; and (**d**) Mean±SE for the number of

steps per Ca^{2+} burst for the initial and trailing Ca^{2+} bursts in tandem events. There is no statistically significance difference between these two values.